

5-1-2014

# Spontaneous Transfer Of Chirality In An Atropisomerically Enriched Two-Axis System

K. T. Barrett

A. J. Metrano

Paul R. Rablen

*Swarthmore College*, prablen1@swarthmore.edu

S. J. Miller

Let us know how access to these works benefits you

Follow this and additional works at: <http://works.swarthmore.edu/fac-chemistry>

 Part of the [Organic Chemistry Commons](#)

---

## Recommended Citation

K. T. Barrett, A. J. Metrano, Paul R. Rablen, and S. J. Miller. (2014). "Spontaneous Transfer Of Chirality In An Atropisomerically Enriched Two-Axis System". *Nature*. Volume 509, Issue 7498. 71-75.  
<http://works.swarthmore.edu/fac-chemistry/102>

This Article is brought to you for free and open access by the Chemistry & Biochemistry at Works. It has been accepted for inclusion in Chemistry & Biochemistry Faculty Works by an authorized administrator of Works. For more information, please contact [myworks@swarthmore.edu](mailto:myworks@swarthmore.edu).



Published in final edited form as:

Nature. 2014 May 1; 509(7498): 71–75. doi:10.1038/nature13189.

## Spontaneous transfer of chirality in an atropisomerically enriched two-axis system

Kimberly T. Barrett<sup>1</sup>, Anthony J. Metrano<sup>1</sup>, Paul R. Rablen<sup>2</sup>, and Scott J. Miller<sup>1,\*</sup>

<sup>1</sup> Department of Chemistry, Yale University, P.O. Box 208107, New Haven, CT 06520-8107.

<sup>2</sup> Department of Chemistry & Biochemistry, Swarthmore College, Swarthmore, PA 19081-1397.

### Abstract

Perhaps the most well-recognized stereogenic elements within chiral molecules are  $sp^3$ -hybridized carbon atoms possessing four different substituents. However, axes of chirality may also exist about bonds with hindered barriers of rotation, leading to stereoisomers known as atropisomers.<sup>1</sup> Understanding the dynamics of these systems can be useful, for example, in the design of single-atropisomer drugs<sup>2</sup> or molecular switches and motors.<sup>3</sup> For molecules that exhibit a single axis of chirality, rotation about that axis leads to racemization as the system reaches equilibrium. We report here a two-axis system in which an enantioselective reaction that produces four stereoisomers (two enantiomeric pairs) displays a more complex scenario. Following a catalytic asymmetric transformation, we observe a kinetically controlled product distribution that is substantially perturbed from the system's equilibrium position. Notably, as the system undergoes isomerization, one of the diastereomeric pairs is observed to drift spontaneously to a higher enantiomeric ratio. In a compensatory manner, the other diastereomeric pair also converts to an altered enantiomeric ratio, reduced in magnitude from the initial ratio. These observations occur within a class of unsymmetrical amides that exhibits two asymmetric axes – one defined through a benzamide substructure, and the other implicit with differentially *N,N*-disubstituted amides. The stereodynamics of these substrates provide an opportunity to observe a curious interplay of kinetics and thermodynamics intrinsic to a system of stereoisomers that is constrained to a situation of partial equilibration.

---

The generation of enantiopure, chiral molecules remains an activity relevant to many scientific fields, from the study of biological systems to materials science. One critical challenge is that enantioenriched compounds are not fully equilibrated ensembles. Enantiopure compounds represent an ensemble of higher free energy due to the entropic

---

Users may view, print, copy, and download text and data-mine the content in such documents, for the purposes of academic research, subject always to the full Conditions of use:[http://www.nature.com/authors/editorial\\_policies/license.html#terms](http://www.nature.com/authors/editorial_policies/license.html#terms)

Correspondence and requests for materials should be directed to S.J.M. ([scott.miller@yale.edu](mailto:scott.miller@yale.edu)).

**Supplementary Information** is available in the online version of the manuscript. Experimental procedures, descriptions of compounds, analytical methods, and computational methods may be found in the Supplementary Information (Sections I-XIV).

**Author Contributions.** S.J.M. and K.T.B. designed the project. K.T.B. performed the experiments. A.J.M. performed the theoretical calculations. All authors contributed to the analysis of data and composition of the manuscript.

**Author Information.** Crystallographic data are deposited with the Cambridge Crystallographic Data Centre under the accession number CCDC 969575 (5-(X-ray)). Reprints and permissions information is available at [www.nature.com/reprints](http://www.nature.com/reprints). The authors declare no competing financial interests.

penalty associated with a one-state, homochiral composition relative to the corresponding two-state racemate.<sup>4</sup> The thermodynamic benefit of a two-state system can counteract asymmetric synthetic efforts, which are commonly performed under kinetic control, in pursuit of single-enantiomer compounds. Examples of racemization familiar to students of chemistry include the isomerization of an enantioenriched  $\alpha$ -chiral aldehyde (Figure 1a) and thermal equilibration of an axially chiral biaryl compound (Figure 1b).<sup>5</sup>

Atropisomerization, the phenomenon of equilibration of stereoisomers about a rotational axis, is an issue of contemporary interest in organic,<sup>6</sup> materials,<sup>7,8</sup> and medicinal chemistry.<sup>9</sup> As part of a program targeted at developing catalysts that produce unique atropisomers selectively, we recently discovered that catalyst **1** is effective for the selective synthesis of enantiomerically enriched benzamides, converting racemic compounds like **2** into the corresponding tribromides (**3**), with enantiomer ratios of up to 94:6 (yields up to 89%; Figure 2).<sup>10</sup> By virtue of a low barrier to racemization of the substrate (**2**), a peptide-catalyzed dynamic kinetic resolution<sup>11</sup> allows for the preferential bromination of one enantiomer, leading to restricted bond rotation and stable atropisomers (**3**) at room temperature for extended periods.

A situation of greater stereochemical intrigue is established when one considers a compound such as **4**. Benzamide **4** (Figure 3), with two different substituents on the amide *N*-atom, may exist as four different stereoisomers (enantiomeric pairs of both *cis*-**4** and *trans*-**4**). Thus, we wondered if it might be possible to identify catalysts that select not only for individual enantiomers, but also for individual diastereomers – each of the four possible stereoisomers (**5**). While peptides such as **1** were envisioned to provide stereochemical control over the atropisomeric axis of **4**, it was unclear at the onset of this study if control of the amide axis disposition (*cis* amide versus *trans* amide) could be accomplished with the same catalyst. If interconversion among all possible diastereomers of the two-axis starting material **4** were possible (with low barriers to isomerization within the starting materials),<sup>12</sup> one could envision four unique catalysts that might accomplish the task. Of course, a critical issue is the overall stability of the individual stereoisomeric products (variants of **5**). Low barriers to rotation about either the benzamide axis (Ar-CO, red bond), the amide bond axis (C-N, blue bond),<sup>13</sup> or both in a concerted manner,<sup>14,15</sup> could conspire to erode kinetic selectivity.

Our studies provided an opportunity to observe a curious result. When *rac*-**4** is exposed to dibromodimethylhydantoin (DBDMH) in the absence of a chiral catalyst, under conditions otherwise analogous to those of Scheme 1 ( $-40\text{ }^{\circ}\text{C}$ ), the expected racemic products are formed over the course of  $\sim 50$  h (70% yield), as a mixture of four stereoisomers (**5**). After the reaction is quenched, the phenol is converted to the methyl ether for analytical purposes to generate **5**-(Me). When the isomeric mixture is purified and analyzed by chiral HPLC ( $\sim 1$  h after quench, at  $25\text{ }^{\circ}\text{C}$ ), the first measurement reveals a ratio of 40:60 ratio *trans*-**5**-(Me):*cis*-**5**-(Me) isomers, each in racemic form (Figure 4a). If the sample is allowed to stand at room temperature (dissolved in 10% *i*PrOH/hexanes) and is re-analyzed at a much later time point (50 h), the *trans*:*cis* ratio is observed to increase to 76:24 (Figure 4b). Notably, while the *cis*-amide of **4** is the minor component of the starting material over a wide temperature range, including at the reaction temperature of  $-40\text{ }^{\circ}\text{C}$ , the *cis*-amide of **5**

(assayed as **5-(Me)**) appears to be generated in slight excess. Thus, it is apparent that there is some modest kinetic selectivity for the *cis*-isomer, which equilibrates at room temperature to the thermodynamically more stable *trans*-amide over time. It is notable that the amide of **5-(Me)** exhibits a barrier to C-N bond isomerization that is high relative to typical amides, but still too low to be effectively arrested at room temperature. The experimental and calculated barriers to C-N bond rotation are determined and discussed below.

When the reaction is performed in the same manner with chiral catalyst **1** (94% yield, within 24 h), a more elaborate scenario is observed. When the product mixture is analyzed by chiral HPLC at the first time point (~ 2 h after quench, at 25 °C), a *trans:cis* ratio of 43:57 is observed (Figure 4c). In this measurement, the *trans*-amide enantiomer ratio (er) is 66:34, while the *cis*-amide er is recorded as 88:12. As the sample is allowed to stand in solution (10% *i*PrOH/hexanes) – long after the chiral catalyst has been removed from the system – the following changes occur spontaneously in the product distribution: At 10 h after quench (Figure 4d), the *trans:cis* ratio moves to 54:46, enhancing the population of the *trans*-isomer as expected. In parallel, the ers of both amide isomers change as the system moves toward the *trans:cis* amide equilibrium position, with the *cis*-amide enantiomer ratio decreasing to 86:14, while the *trans*-amide er spontaneously increases to 72:28. These changes continue as the system continues to equilibrate. At 24 h (Figure 4e), the *trans:cis* ratio is 68:32; the *cis*-amide er erodes to 84:16, while the *trans*-amide er increases to 77:23. At the 72 h mark, the product ratios have stabilized (Figure 4f), and the apparent equilibrium position of the amide diastereomers has been reached, with a *trans:cis* ratio of 76:24. At this stage, the *cis*-amide er is 79:21, equivalent to the *trans*-amide er, also 79:21. These observations are depicted graphically in Figure 4g. While data are shown in Figure 4 for reactions conducted at –40 °C, the observations are qualitatively reproduced when the experiments are repeated at several different temperatures (see Supplementary Information, Section VIIa).

Our observations reflect a situation of spontaneous enantioenrichment for one of the product diastereomers (*trans*), with a compensatory decrease in er for the other diastereomer (*cis*). Interestingly, a 50:50 racemic mixture *is not* observed, with the system retaining enantioenrichment even after prolonged periods of time at room temperature, a consequence of the two-axis system failing to reach complete equilibrium within the time frame analyzed (*vide infra*).

Both the *trans* and the *cis* isomers of the products could be separated by silica gel chromatography – a rather unusual circumstance – and each produced the expected diastereomeric *trans:cis* ratio (76:24) upon standing in solution (10% *i*PrOH/hexanes). In these cases, the er of the samples remains virtually constant (*cis*, 87:13; *trans*, 74:26; See Sections VIc and VI d and Figure S7 in the Supplementary Information for details).

Through separation of the enantioenriched *cis*- and *trans*-amide isomers, enantioenriched *trans*-material was obtained and provided crystallographic quality material to assign (*S*, *trans*)-**5** as the major isomeric component after amide equilibration (Figure 4h; see also, Supplementary Information, Section IV). It is interesting to note that the stereoisomer obtained for assignment of the *S-trans* configuration was derived from isolation of the *cis* product, reflecting the crystallization of the major *trans* diastereomer, as *cis*-to-*trans*

equilibration occurs over the course of the crystallization experiment. Parenthetically, the absolute configuration of this *S-trans* sample, derived from the isolation of enriched *cis* sample, is the same absolute configuration observed when catalyst **1** operates on substrate **2**, to deliver enantioenriched (**S-3**) with a 94:6 er (Figure 2).<sup>10</sup> Accordingly, these data provide circumstantial support for the equilibration of the *S-cis* isomer to the *S-trans* isomer (and of *R-cis* to *R-trans* also) without interconversion of the axis of chirality. Further details of this scenario are now considered below.

As *cis*-to-*trans* amide isomerization occurs and the diastereomeric ratio reaches its equilibrium position, the final ers for both the *trans*-amide isomers and the *cis*-amide isomers emerge as equivalent. As is implicit in Figure 4g, the sum of the major enantiomer of each amide diastereomer (**S-cis-5-Me** + **S-trans-5-Me**), divided by the sum of the minor enantiomer for each diastereomeric amide (**R-cis-5-Me** + **R-trans-5-Me**) is near 79:21 (3.76 ± 0.41) at each time point in Figure 4 (Table S6 and Figure S5 of the Supplementary Information contain expanded data sets detailing this point). The convergence of the er for both the *trans*- and *cis*-amide diastereomers is consistent with a mechanistic model wherein amide isomerization occurs through independent C-N bond rotation at ambient temperature (Figure 3), while the enantiomer-defining axis of chirality (Ar-CO) is essentially fixed. The equilibration of the amide isomers, without interconversion of the Ar-CO bond axis, leads to fluctuation of the starting *cis*-amide er downward, and the *trans*-amide er upward, until amide isomerization achieves the equilibrium ratio, and the ers of the diastereomers are equivalent.

However, when the *cis*- or *trans*-amide diastereomers are separated by chromatography, and the isolated amide diastereomers are allowed to re-equilibrate, the er remains constant in each series. This situation is once again a manifestation of the  $\Sigma(S\text{-}cis + S\text{-}trans) / \Sigma(R\text{-}cis + R\text{-}trans)$  remaining constant. In this case, there is no reservoir of the other amide diastereomer, of a different er, to distribute its population of either *S*- or *R*-configuration differentially to the two amide diastereomers at the C-N bond equilibrium position.

To explore the plausibility of these assertions, we complemented our experiments with a series of DFT calculations to ascertain the barriers associated with the critical modes of isomerization. The dynamics described above for amide isomerization correspond to experimentally derived free energies barriers<sup>17,18</sup> of 24.8 kcal/mol (*trans*-to-*cis*) and 24.1 kcal/mol (*cis*-to-*trans*) (Figure 5; see Supplementary Information, Section VIII). Computations<sup>19,20</sup> provided free energy barriers of 24.4 kcal/mol (*trans*-to-*cis*) and 24.0 kcal/mol (*cis*-to-*trans*) respectively (Supplementary Information, Section XIII), on par with both the experimentally determined values and literature values for somewhat related compounds.<sup>13</sup> Additionally, during the entire computed C-N rotation process, the Ar-CO dihedral angle remains close to its value in the ground state, even as the amide axis rotates out of conjugation with the carbonyl and pyramidalizes (**TS-5a**, Figure 5b). Thus, independent C-N bond rotation appears to have a much lower barrier than any putative process involving a coupled rotation of the Ar-CO axis. This is consistent with the observation that erosion of the overall enantioenrichment of the system does not occur at room temperature.<sup>21,22</sup>

Of interest to the present system are previous reports by Clayden, which showed that rotations about the Ar-CO bond axis of sterically hindered tertiary amides follow a mechanistic course involving concerted rotations of the Ar-CO axis and the amide C-N bond axis, in a gearing fashion, when sufficient energy is available to the system.<sup>21,23</sup> Our calculations for the present system reassert these conclusions. However, the system we present here is distinct in that (a) the action of a chiral catalyst delivers diastereomeric amides of different *er* that allows for the observation of fluctuating enantiomeric ratios, and (b) distinct steric demands of the substrate that separate the energetic barriers of geared Ar-CO/C-N isomerization from independent C-N bond rotation substantially. Computations employing a relaxed potential energy scan of the Ar-CO dihedral angle led to a simultaneous rotation about the amide C-N bond. The optimized transition states along this torsional energy profile were marked by non-coplanar *N*- and aryl-substituents and imaginary frequencies that showed coupled rotation about both axes. Compared to independent Ar-CO rotation, which suffers from an implausibly high computed barrier, this concerted Ar-CO/C-N rotation represents the lowest energy pathway to inversion of the atropisomeric axis (**TS-5b**, Figure 6a). However, below these energetic thresholds, our results with compound **5** are consistent with independent C-N rotation, as noted above.

While amide isomerization occurred at ambient temperatures, we could induce racemization only through heating the atropisomeric benzamides at elevated temperatures (toluene, > 60 °C). We determined the free energy barrier to racemization experimentally,<sup>24</sup> and found a value of 27.8 kcal/mol (at 70 °C) for the *cis*-**5**(Me) isomer, and a value of 28.6 kcal/mol for the lower energy *trans*-**5**(Me) isomer (Figure 6b; see Supplementary Information, Section IX). When the barriers were computed, values of 28.2 kcal/mol and 28.5 kcal/mol for *cis*-**5**(Me) and *trans*-**5**(Me) were found respectively, in good accord with the experimentally determined values and literature precedent (see Supplementary Information, Section XIV).<sup>25</sup> Taken together, our results imply that the racemization pathway involves, for a given amide diastereomer (e.g., (*S*, *trans*)-**5**(Me) to (*R*, *trans*)-**5**(Me)): (a) a concerted motion of the Ar-CO/C-N axes to convert (*S*, *trans*)-**5**(Me) to (*R*, *cis*)-**5**(Me); (b) an independent motion of the C-N axis converting (*R*, *cis*)-**5**(Me) to (*R*, *trans*)-**5**(Me), as the original amide diastereomer is restored (Figure 6a). Based on the experiments and calculations above, it appears that the concerted two-axis rotation is operative at elevated temperature, and exhibits a high enough barrier such that it is prohibitively slow at room temperature.

In summary, we have observed a stereoisomeric system in which spontaneous enantiomeric enrichment occurs in homogeneous solution, with a compensatory erosion of *er* in a coupled diastereomer. The observation is made possible by the formation of a nonequilibrium mixture of amide diastereomers, wherein each enantiomeric pair is produced under the kinetic influence of a chiral catalyst. Amide isomerization occurs with fluctuation of each diastereomer's *er* as *cis/trans* amide equilibration occurs; yet, the chirality-defining element does not enantiomerize. Instead, the overall enantioenrichment of the system is retained as the populations of each isomer interconvert. Our understanding of the dynamic processes includes an assessment of the intrinsic barriers for the isomerizations, as a function of individual bond rotations, or those that may occur in a concerted manner. The interconversion of stereoisomers in the presence of a fixed element of chirality has been



exploited to great advantage in the development of asymmetric reactions.<sup>26,27</sup> Yet, the present case of fluctuating enantiomeric ratios, without epimerization of a chiral element within reaction products that have been isolated away from their equilibrium positions, is distinct. These features may be of interest given the current literature on atropisomerization.<sup>28,29</sup> Moreover, these observations may inform endeavors where spontaneous transfer of chirality occurs among the components of a system as a function of the interplay of kinetics and thermodynamics.<sup>30</sup>

## Methods Summary

Dibromodimethylhydantoin (DBDMH, 85.8 mg, 0.30 mmol) was added to a 0.02 M solution of the aromatic amide **4** (66.9 mg, 0.20 mmol) and catalyst **1**<sup>10</sup> (11.5 mg, 0.02 mmol) in CHCl<sub>3</sub> (10 mL) at various temperatures (0 °C, -40 °C, or -55 °C). The reaction was allowed to stir overnight (15-22 h). The reaction was then quenched with a 1.5 M solution of butyl vinyl ether in methanol (MeOH, 0.5 mL). The time of quench was recorded for amide equilibration calculations and defined as time zero (see Supplementary Information Section VIII). For ease of chiral HPLC development, the phenol was subsequently protected as the methyl ether. The reaction was allowed to warm to room temperature and additional methanol was added (2.0 mL, ~5:1 by volume CH<sub>2</sub>Cl<sub>2</sub>:MeOH) followed by 2.0 M trimethylsilyldiazomethane in hexanes (0.4 mL). The methylation was quenched with silica gel upon completion (15-30 min), filtered, and concentrated under reduced pressure. Flash chromatography of the crude residue with hexanes/EtOAc afforded products (as a *cis/trans* mixture or independently isolated isomers). This material (**5-Me**) was dissolved in a 10% *isopropanol*/hexanes mixture (0.1 M) and allowed to equilibrate, in solution, at room temperature over a prolonged time course to determine the experimental barriers to amide isomerization. Barriers to racemization of **5-Me** were determined experimentally by heating in toluene at 70 °C (0.6 M). Isomeric ratios were determined by chiral HPLC utilizing a Chiralcel OD-H column, with a flow rate of 0.75 mL/min, in 95:5 hexanes:ethanol:  $R_{T(r, trans)} = 14.0$  min,  $R_{T(s, trans)} = 15.3$  min,  $R_{T(s, cis)} = 20.6$  min,  $R_{T(r, cis)} = 23.9$  min.

## Supplementary Material

Refer to Web version on PubMed Central for supplementary material.

## Acknowledgements

We are grateful to the National Institute of General Medical Sciences of the NIH (GM-068649) for support. We also wish to thank Louise Guard for X-ray crystallography. A.J.M. was supported by the National Science Foundation Graduate Research Fellowship Program. All computational work was supported by the facilities and staff of the Yale University Faculty of Arts and Sciences High Performance Computing Center, and by the National Science Foundation under grant #CNS 08-21132 that partially funded acquisition of the facilities.

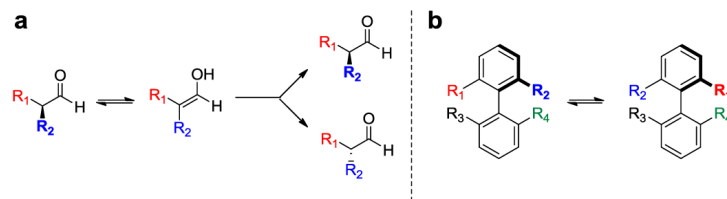
## References

1. Oki M. Topics in Stereochemistry. 1983; 1
2. Clayden J, Moran WJ, Edwards PJ, LaPlante SR. The challenge of atropisomerism in drug discovery. Angew. Chem. Int. Edn. 2009; 48:6398–6401.
3. Feringa BL. The art of building small: from molecular switches to molecular motors. J. Org. Chem. 2007; 72:6635–6652. [PubMed: 17629332]

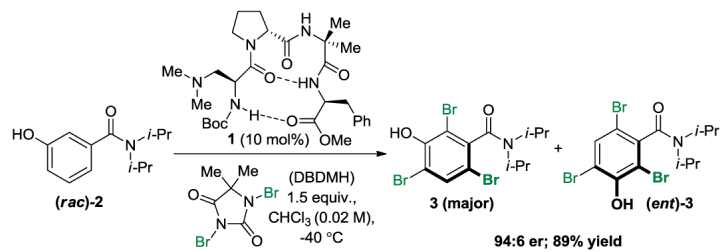
4. Eliel, EL.; Wilen, S. Stereochemistry of organic compounds. Wiley Interscience; New York: 1994. p. 425
5. Reist M, Testa B, Carrupt P-A, Jung M, Schurig V. Racemization, diastereomerization, and epimerization: their meaning and pharmacological significance. *Chirality*. 1995; 7:396–400.
6. Reichert S, Breit B. Development of an axial chirality switch. *Org. Lett.* 2007; 9:899–902. [PubMed: 17284047]
7. Wang J, B.L. Feringa. Dynamic control of chiral space in a catalytic asymmetric reaction using a molecular motor. *Science*. 2011; 331:1429. [PubMed: 21310964]
8. Kelly TR, De Silva H, Silva RA. Unidirectional rotary motion in a molecular system. *Nature*. 1999; 401:150–152. [PubMed: 10490021]
9. LaPlante SR, et al. Assessing atropisomer axial chirality in drug discovery and development. *J. Med. Chem.* 2011; 20:7005–7022. [PubMed: 21848318]
10. Barrett KT, Miller SJ. Enantioselective synthesis of atropisomeric benzamides through peptide-catalyzed bromination. *J. Am. Chem. Soc.* 2013; 135:2963–2966. [PubMed: 23410090]
11. Keith JM, Larrow JF, Jacobsen EN. Practical considerations in kinetic resolution reactions. *Adv. Synth. & Catal.* 2001; 343:5–26.
12. Cox C, Lectka T. Synthetic catalysis of amide isomerization. *Acc. Chem. Res.* 2000; 33:849–858. [PubMed: 11123884]
13. Mannschreck A, Mattheus A, Rissmann G. Comparison of kinetic results obtained by NMR line shape and equilibration methods. *J. Mol. Spec.* 1967; 23:15–31.
14. Ahmed A, Bragg RA, Clayden J, Lai L-W, McCarthy C, Pink JH, Westlund N, Yasin SA. Barriers to rotation about the chiral axis of tertiary aromatic amides. *Tetrahedron*. 1998; 54:13277–13294.
15. Iwamura H, Mislow K. Stereochemical consequences of dynamic gearing. *Acc. Chem. Res.* 1988; 21:175–182.
16. Bringmann G, Price Mortimer AJ, Keller PA, Gresser MJ, Garner J, Breuning M. Atroposelective synthesis chiral biaryl compounds. *Angew. Chem. Int. Ed.* 2005; 44:5384–5427.
17. Erol S, Dogan I. Determination of barriers to rotation of axially chiral 5-methyl-2-(o-aryl)imino-3-(o-aryl)thiazolidine-4-ones. *Chirality*. 2012; 24:493–498. [PubMed: 22553079]
18. Chupp JP, Olin JF. Chemical and physical properties of some rotational isomers of  $\alpha$ -haloacetanilides, a novel unreactive halogen system. *J. Org. Chem.* 1967; 32:2297–3303.
19. Zhao Y, Truhlar DG. The M06 suite of density functionals for main group thermochemistry, thermochemical kinetics, noncovalent interactions, excited states, and transition elements: two new functionals and systematic testing of four M06-class functionals and 12 other functionals. *Theor. Chem. Acc.* 2008; 120:215–41.
20. Campomanes P, Menendez, Sordo TL. A theoretical analysis of enantiomerization in aromatic amides. *J. Phys. Chem.* 2002; 106:2623–2628.
21. Bragg RA, Clayden J, Morris GA, Pink JH. Stereodynamics of bond rotation in tertiary aromatic amides. *Chem Eur. J.* 2002; 8:1279–1289. [PubMed: 11921211]
22. Pirkle WH, Welch CJ, Zych AJ. Chromatographic investigation of the slowly interconverting atropisomers of hindered naphthamides. *J. Chromatography*. 1993; 648:101–109.
23. Clayden J, Pink JH. Concerted rotation in a tertiary aromatic amide: toward a simple molecular gear. *Angew. Chem. Int. Ed.* 1998; 37:1937–1939.
24. Eliel, EL.; Wilen, S. Stereochemistry of organic compounds. Wiley Interscience; New York: 1994.
25. Cuyegkeng MA, Mannschreck A. Chromatographic separation of enantiomers and barriers to enantiomerization of axially chiral aromatic carboxamides. *Chem Ber.* 1987; 120:803–809.
26. Lee WK, Park YS, Beak P. Dynamic thermodynamic resolution: advantage by separation of equilibration and resolution. *Acc. Chem. Res.* 2009; 42:224–234. [PubMed: 19152329]
27. Hirsch R, Hoffmann RW. A test on the configurational stability of chiral organolithium compounds based on kinetic resolution; scope and limitations. *Chem. Ber.* 1992; 125:975–982.
28. LaPlante SR, Edwards PJ, Fader LD, Jakalian A, Hucke O. Revealing atropisomer axial chirality in drug discovery. *ChemMedChem*. 2011; 3:505–513. [PubMed: 21360821]



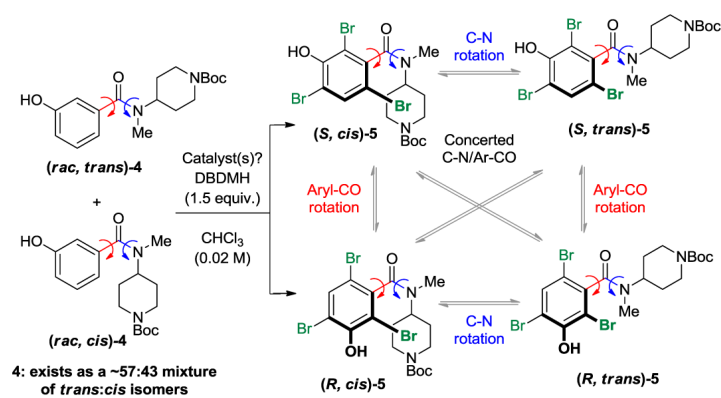
29. LaPlante R, et al. Enantiomeric atropisomers inhibit HCV polymerase and/or HIV matrix: characterizing hindered bond rotations and target selectivity. *J. Med. Chem.* ASAP. 2013 Doi: 10.1021/jm401202a.
30. Klussman M, et al. Thermodynamic control of asymmetric amplification in amino acid catalysis. *Nature*. 2006; 441:621–623. [PubMed: 16738656]



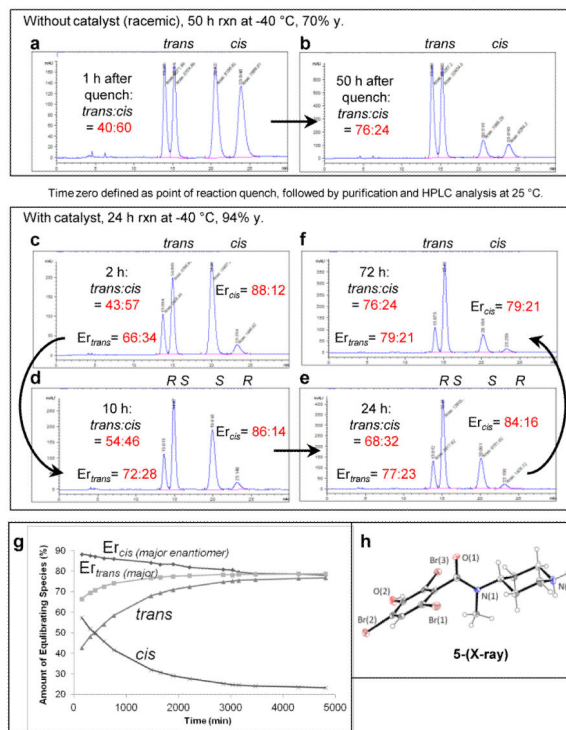
**Figure 1.** Stereochemical interconversion of chiral organic compounds. **a**, Racemization of an enantioenriched  $\alpha$ -substituted aldehyde. **b**, Atropisomerization of an axially chiral biaryl compound.



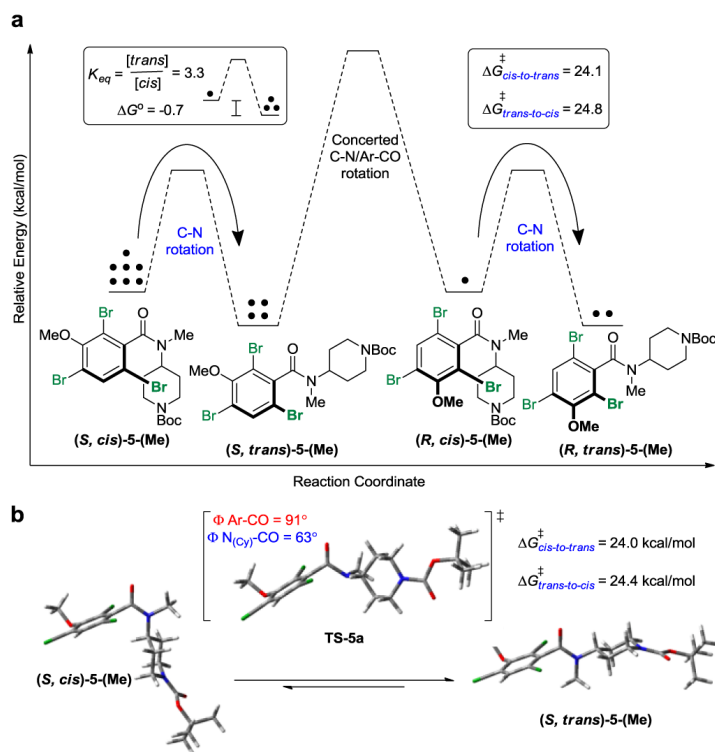
**Figure 2.**  
Catalytic enantioselective bromination of *N,N*-diisopropyl benzamides.



**Figure 3.** Proposed catalytic enantioselective bromination of a two-axis, differentially substituted benzamide. [The use of the R- and S-stereochemical descriptors are in accord with convention, and are defined interchangeably with the also-used M- and P-stereochemical convention. R = M; S = P.]<sup>16</sup>

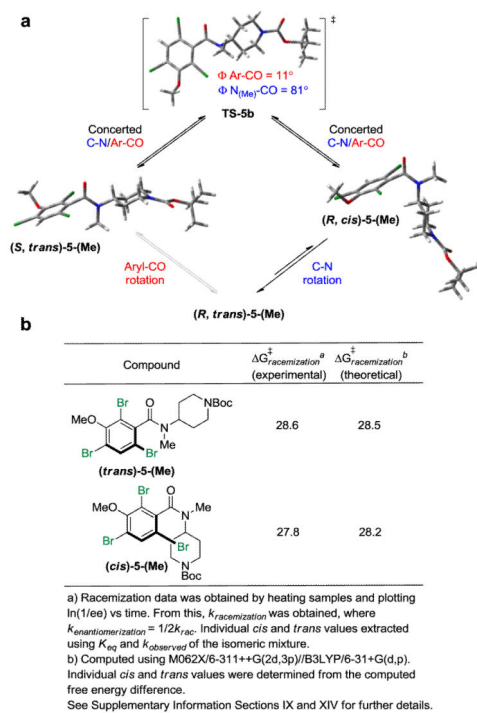
**Figure 4.**

Experimental data describing the stereochemical behavior of the isomeric benzamide products. **a-f:** Chiral HPLC traces of **5-(Me)** analyzed at r.t. (**a-b**, reactions run at -40 °C in the absence of catalyst; **c-f**, in the presence of catalyst and subsequently monitored over time after reaction work-up.) Peak assignments in order of elution: peak 1: *R*, *trans*; peak 2: *S*, *trans*; peak 3: *S*, *cis*; peak 4: *R*, *cis*. **g**, Graphical representation of changes in isomeric components. **h**, Crystallographic structure of (*S*, *trans*)-derivative used for the absolute stereochemistry assignments.<sup>16</sup>



**Figure 5.** Energetic considerations and analysis of the stereoisomerizations. **a**, Energy diagram representing the initial experimental isomeric populations, equilibrium populations (inset 1), and experimentally derived amide rotational barriers (inset 2) of **5-(Me)** at 25 °C (10% *i*PrOH/Hexanes). **b**, Computed ground states and transition state geometries for amide isomerization of (*S*)-**5-(Me)**. Computations were performed with a torsional potential energy scan of the C-N dihedral angle, followed by geometry optimization of all stationary points (transition states and minima) using B3LYP/6-31+G(d,p). Harmonic vibrational frequencies were calculated at the same level of theory in order to determine free energies ( $G$ ), and single point energies were computed using M06-2X/6-311++G(2d,3p).



**Figure 6.**

Energetic considerations and analysis of racemization dynamics. **a**, Computed geometries and modes of isomerization of **5-(Me)** with a concerted C-N/Ar-CO rotation and independent C-N rotation leading to racemization at high temperatures. **b**, Experimentally and theoretically calculated barriers to racemization of atropisomeric benzamides.